Article:
Fairbairn, AI and Kelmanson, MA (2018) Error analysis of a spectrally accurate Volterra-transformation method for solving 1-D Fredholm integro-differential equations. International Journal of Mechanical Sciences, 144. pp. 382-391. ISSN: 0020-7403

https://doi.org/10.1016/j.ijmecsci.2018.04.052

Error analysis of a spectrally accurate Volterra-transformation method for solving 1-D Fredholm integro-differential equations

Abigail I Fairbairn, Mark A Kelmanson

PII: S0020-7403(18)30482-X
DOI: 10.1016/j.ijmecsci.2018.04.052
Reference: MS 4307

To appear in: *International Journal of Mechanical Sciences*

Received date: 10 February 2018
Accepted date: 28 April 2018

Please cite this article as: Abigail I Fairbairn, Mark A Kelmanson, Error analysis of a spectrally accurate Volterra-transformation method for solving 1-D Fredholm integro-differential equations, *International Journal of Mechanical Sciences* (2018), doi: 10.1016/j.ijmecsci.2018.04.052

Error analysis of a spectrally accurate Volterra-transformation method for solving 1-D Fredholm integro-differential equations

Logarithmic plots demonstrating not only the impressive agreement between computed N-node actual errors e_N (small symbols) with bounds b_N (large symbols) predicted by new theory, but also the improvement of accuracy relative to part 1 of the new theory (crosses).

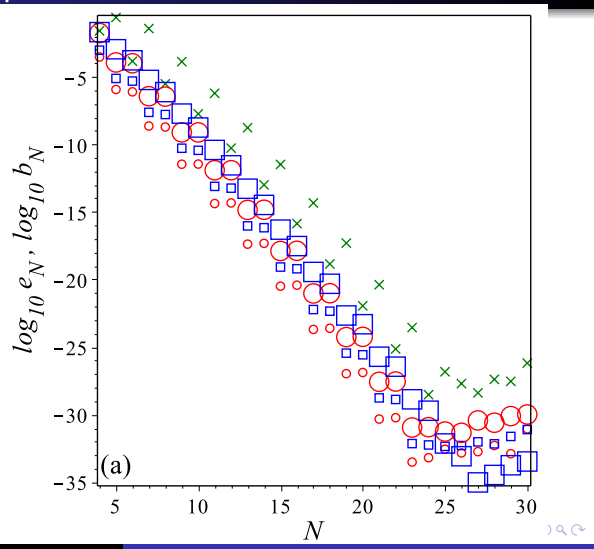

Abigail I Fairbairn and Mark A Kelmanson *Int. J. Mech. Sci.* (2018)

Highlights

- New explicit formulae fora priori errors boundsvia abstract operator theory
- Bounds obtained using computer algebra using only the inherent numerical solution
- True errors approximated to spectral accuracy by new bounds
- Volterra transformation bypasses numerical differentiation, improving accuracy

Error analysis of a spectrally accurate Volterra-transformation method for solving 1-D Fredholm integro-differential equations

Abigail I Fairbairn and Mark A Kelmanson*

Department of Applied Mathematics, University of Leeds, Leeds LS2 9JT, UK

Abstract

Spectrally accurate *a priori* error estimates for Nyström-method approximate solutions of one-dimensional Fredholm integro-differential equations (FIDEs) are obtained indirectly by transforming the FIDE into a hybrid Volterra-Fredholm integral equation (VFIE), which is solved via a novel approach that utilises N-node Gauss-Legendre interpolation and quadrature for its Volterra and Fredholm components respectively. Errors in the numerical solutions of the VFIE converge to zero exponentially with N, the rate of convergence being confirmed via large-N asymptotics. Not only is the exponential rate far superior to the algebraic rate achieved in previous literature [29] but also it is demonstrated, via diverse test problems, to improve dramatically on even the exponential rate achieved in the approach [21] of direct Nyström discretisation of the original FIDE; this improvement is confirmed theoretically.

Keywords: Integro-ordinary differential equations, error bounds, spectral, collocation and related methods
2010 MSC: 45J05, 65L70, 65M70

1. Introduction

In the substantial literature on the approximation of solutions of one-dimensional Fredholm integro-differential equations (FIDEs), corresponding error analyses are notably scarce. For example, though the independent studies (in chronological order) [38, 4, 39, 28, 5, 15, 34, 40, 8, 31, 2, 1, 22, 35] present diverse FIDE-solution techniques of varying degrees of efficiency and (disparate) accuracy, only [28, 40, 31, 1] include a discussion of errors and, in even these cases, error analyses are limited (see summary in [21, §1]) to estimates of convergence rates: that is, the direct computation of theoretically predicted error bounds is almost entirely absent.

The present work is therefore motivated on two fronts: to develop not only a novel numerical method that converges exponentially in the dimension N of the discrete numerical method, but also an explicit error analysis that is implementable and yields errors in terms of only the computed numerical solution. In [21], the authors develop a novel approach for achieving these two goals, but the method developed therein—based on a combination of numerical quadrature and numerical differentiation—has a global error dictated

*Corresponding author email address: M.Kelmanson@leeds.ac.uk

by the latter process, which is considerably less accurate than the former because of the ill-conditioning of its inherent differentiation matrix. Accordingly, an approach independent of [21] is presently pursued in which the need for numerical differentiation is circumvented by first transforming the FIDE (as in, e.g., [29]) into a Volterra-Fredholm integal equation (VFIE); though the solution of this can be approximated in a number of ways (see, e.g., [26, 16, 13, 9, 33]), a different approach, first explored by the authors in [19], is adopted herein.

The remainder of this paper is structured as follows. In §2 is presented an FIDE-to-VFIE conversion approach in [29], in which the VFIE is solved to (only; see below) *quadratic* order in the number N of Simpson's-rule panels used. In §3 the VFIE is solved numerically to *spectral* order in N, the degree of the highest-order orthogonal polynomial used in the approximation of the VFIE solution. This approach obviates the need for the numerical differentiation matrices, used in a companion paper [21], the ill-conditioning of which is reviewed and analysed in §3.1. In §4 is presented a novel error analysis, for the VFIE numerical solution procedure, whose distinctive aspect is computation of the error in the numerical solution of the original FIDE *explicitly* in terms of the numerical approximation of the derivate that results from the VFIE reformulation. In §5 numerical results of test problems, some challenging, are presented that validate to spectral accuracy both the implementation outlined in §3 and the error analysis of §4. Brief conclusions are presented in §6.

2. Conversion from FIDE to VFIE

The canonical form on the normalised interval $[-1,1]$ of the first-order one-dimensional Fredholm integro-differential equation (FIDE) for the unknown function $u(x)$ is

$$u(x) - \mu(x)\,\frac{du}{dx}(x) - \lambda \int_{-1}^{1} K(x,y)\,u(y)\,dy = f(x)\,, \quad x \in [-1,1]\,, \tag{1}$$

in which the source function $f : [-1,1] \to \mathbb{R}$, the kernel $K : [-1,1] \times [-1,1] \to \mathbb{R}$ and coefficient function $\mu : [-1,1] \to \mathbb{R}$ are prescribed functions of $x, y \in [-1,1]$ and the parameter $\lambda \in \mathbb{R}$ is a constant. By hypothesis, (1) is solvable and so $u(x)$ exists. In symbolic form, (1) is

$$u - \mu\,\mathcal{D}\,u - \lambda\,\mathcal{K}\,u = f\,, \tag{2}$$

where $u,\ f \in \mathcal{C} \equiv C[-1,1]$, the Banach space with supremum norm $\|\cdot\|$ on which the action of the differential operator $\mathcal{D}$ on u is defined by

$$\mathcal{D}\,u = (\mathcal{D}\,u)(x) \equiv u'(x)\,,$$

wherein a prime denotes differentiation with respect to x. The action in (2) of the compact integral operator $\mathcal{K}$ on u is defined by

$$\mathcal{K}\,u = (\mathcal{K}\,u)(x) \equiv \int_{-1}^{1} K(x,y)\,u(y)\,dy\,.$$

The FIDE (1) is augmented by the boundary condition (BC)

$$u(\xi) = \zeta, \quad \xi \in [-1, 1]\,, \tag{3}$$

i.e. ξ is a prescribed real constant in the interval containing all Legendre nodes.When the BC is given for $\xi = \pm 1$, the FIDE can be converted into a Volterra-Fredholm integral equation (VFIE) following the approach in, e.g., [29]; the details of this conversion for $\xi = -1$ are as follows. Define the function $v(x)$ by

$$v(x) \equiv u'(x)\,, \tag{4}$$

integration of which, upon using (3), yields

$$u(x) = \zeta + \int_{-1}^{x} v(y)\, dy\,, \tag{5}$$

whence the FIDE (1) becomes

$$\zeta + \int_{-1}^{x} v(y)\, dy - \mu(x)\, v(x) - \lambda \int_{-1}^{1} K(x,y) \left(\zeta + \int_{-1}^{y} v(z)\, dz\right) dy = f(x)\,. \tag{6}$$

By the existence of $u(x)$ and (5), $v(x)$ is integrable, hence the order of double integration in the final term on the right-hand side of (6) can be exchanged, thereby rendering (6) as the VFIE

$$v(x) = g(x) + \frac{1}{\mu(x)} \int_{-1}^{x} v(y)\, dy - \lambda \int_{-1}^{1} k(x,y)\, v(y)\, dy\,, \tag{7}$$

in which the modified source function $g(x)$ is given by

$$g(x) = \frac{1}{\mu(x)} \left(\zeta - \lambda\, \zeta \int_{-1}^{1} K(x,y)\, dy - f(x)\right)\,,$$

and the modified kernel $k(x,y)$ by

$$k(x,y) = \frac{1}{\mu(x)} \int_{y}^{1} K(x,z)\, dz\,. \tag{8}$$

By defining the action of the (Volterra) integral operator $\mathcal{V}$ on $v \in \mathcal{C}$ by

$$\mathcal{V}\, v = (\mathcal{V}\, v)(x) \equiv \int_{-1}^{x} v(y)\, dy\,, \tag{9}$$

and that of the (Fredholm) integral operator $\mathcal{F}$ on $v \in \mathcal{C}$ by

$$\mathcal{F}\, v = (\mathcal{F}\, v)(x) \equiv \int_{-1}^{1} k(x,y)\, v(y)\, dy\,, \tag{10}$$

the symbolic form of the VFIE (7) corresponding to FIDE (2) is

$$v = g + \frac{\mathcal{V}\, v}{\mu} - \lambda\, \mathcal{F}\, v\,. \tag{11}$$

The FIDE-to-VFIE conversion for the case when the BC is at $x = 1$ follows analogously by replacing integrals $\int_{-1}^{x}$ with $\int_{x}^{1}$ in (5), (6), (7) and (9) and replacing $\int_{y}^{1}$ with $\int_{-1}^{y}$ in (8).

The original FIDE (2) can now be solved via (5) and (7) without the need for numerical differentiation. The symbolic equation (11) will form the basis of the error analysis in section §4.

3. Numerical Solution of the VFIE

Let $y_{j,N},\ j = 1, \ldots, N$ be a set of N distinct nodes in $[-1, 1]$ ordered so that $-1 \leq y_{1,N} < y_{2,N} < \ldots < y_{N-1,N} < y_{N,N} \leq 1$, using which the action of the N-node Lagrange-interpolation operator $\mathcal{L}_N$ on $v \in \mathcal{C}$ is defined as

$$\mathcal{L}_N\, v = (\mathcal{L}_N\, v)(x) \equiv \sum_{j=1}^{N} L_{j,N}(x)\, v(y_{j,N})\,, \tag{12}$$

wherein the Lagrange basis functions are given by

$$L_{j,N}(x) = \prod_{\substack{l=1 \\ l \neq j}}^{N} \frac{x - y_{l,N}}{y_{j,N} - y_{l,N}}, \quad j = 1, \ldots, N\,. \tag{13}$$

To approximate the Volterra term in (11), define the (Volterra-Lagrange) operator $\mathcal{V}_N \equiv \mathcal{V}\,\mathcal{L}_N$. Application of the operator $\mathcal{V}$ to both sides of the approximate Lagrange interpolation $v \approx \mathcal{L}_N\, v$ then yields

$$\mathcal{V}\, v \approx \mathcal{V}_N\, v = (\mathcal{V}_N\, v)(x) \equiv \sum_{j=1}^{N} \tau_{j,N}(x)\, v(y_{j,N})\,, \tag{14}$$

in which

$$\tau_{j,N}(x) = \mathcal{V}\, L_{j,N}(x)\,, \quad j = 1, \ldots, N\,.$$

To approximate the Fredholm term in (11), define the (Fredholm-Gauss) operator $\mathcal{F}_N$ that approximates the action of $\mathcal{F}$ by the Nyström quadrature

$$\mathcal{F}\, v \approx \mathcal{F}_N\, v = (\mathcal{F}_N\, v)(x) \equiv \sum_{j=1}^{N} w_{j,N}\, k(x, y_{j,N})\, v(y_{j,N})\,, \tag{15}$$

in which $w_{j,N}$ and $y_{j,N}$ are respectively the weights and abscissae of the Gaussian integration rule. As the weight function in the integral (10) for $\mathcal{F}\, v$ is unity, the nodes $y_{j,N}$ can be chosen as Gauss-Legendre, Legendre-Gauss-Radau or Legendre-Gauss-Lobatto distributions. Via (14) and (15), the discrete approximation of VFIE (7) is obtained as

$$v_N(x) = g(x) + \sum_{j=1}^{N} \left\{ \frac{\tau_{j,N}(x)}{\mu(x)} - \lambda\, w_{j,N}\, k(x, y_{j,N}) \right\} v_N(y_{j,N}) \tag{16}$$

which, when collocated at nodes $x = y_{i,N},\ i = 1, \ldots, N$, yields the $N \times N$ linear system

$$(\mathbf{I}_N - \mathbf{M}_N)\, \mathbf{v}_N = \mathbf{g}_N\,. \tag{17}$$

The matrix and vector entries in (17) are given by, for $i, j = 1, \ldots, N$,

$$\{\mathbf{I}_N\}_{i,j} = \delta_{ij}\,, \quad \{\mathbf{M}_N\}_{i,j} = \frac{\tau_{j,N}(y_{i,N})}{\mu(y_{i,N})} - \lambda\, w_{j,N}\, k(y_{i,N}, y_{j,N})\,,$$

$$\{\mathbf{v}_N\}_i = v_N(y_{i,N}) \quad \text{and} \quad \{\mathbf{g}_N\}_i = g(y_{i,N})\,, \tag{18}$$

wherein δ_{ij} is the Kronecker delta. Inversion of (17) yields the N nodal values $v_N(y_{i,N})$ which, when substituted into the inversion formula (16), give the approximate solution $v_N(x)$ of (7), which in symbolic form is

$$v_N = g + \frac{\mathcal{V}_N v_N}{\mu} - \lambda \mathcal{F}_N v_N. \tag{19}$$

Note that computing $v_N(x)$ directly via the inversion formula (16) is more accurate [18] than using Lagrange interpolation (12). By (5), the exact solutions v and u, of the VFIE and FIDE respectively, satisfy the symbolic equation

$$u = \zeta + \mathcal{V}\, v\,, \tag{20}$$

to which application of $\mathcal{D}$ to both sides yields $\mathcal{D}\, u = \mathcal{D}\, \mathcal{V}\, v$, i.e. $v = \mathcal{D}\, \mathcal{V}\, v$, so that $(\mathcal{D})^{-1} = \mathcal{V}$. Additionally, (20) implies that there are two cases to consider when recovering the numerical solution u_N from its derivative v_N computed via (17)–(19). First, if $v_N(x)$ is exactly integrable (case 1) then the approximate numerical solution u_N of (2) can be computed from v_N as

$$\widetilde{u}_N = \zeta + \mathcal{V}\, v_N\,. \tag{21}$$

Second, if functions $\mu(x)$, $K(x,y)$ and $f(x)$ in IDE (1) are such that (19) is not exactly integrable (case 2) then the approximate numerical solution u_N of (2) must in this case be computed from v_N as

$$\widehat{u}_N = \zeta + \mathcal{V}_N\, v_N, \tag{22}$$

which yields $\widehat{u}_N(x)$ as a polynomial of degree N in x. Note that this method requires only (17)–(18), as $v_N(x)$ does not need to be computed via (19) since only its nodal values, given by the solution vector $\mathbf{v}_N$ of (17), are present in the last term in (22).

3.1. Digression: ill-conditioned differentiation matrices

For completeness, circumvention of the use of numerical differentiation (as employed in [21]) is now discussed. The action of the differentiation operator $\mathcal{D}$ in (2) is approximated by the operator $\mathcal{D}_N$, with

$$\mathcal{D}u \approx \mathcal{D}_N u = \sum_{j=1}^{N} L'_{j,N}(x)\, u(y_{j,N})\,, \tag{23}$$

in which the Lagrange-basis function $L_{j,N}(x)$ is defined in (13), the nodes $y_{j,N},\ j = 1, \ldots, N$ are defined at the opening of §3, and a prime denotes differentiation with respect to x.

It is well-known that, when the node set are the roots of orthogonal polynomials, for suitable functions u the action of $\mathcal{D}$ is approximated to spectral accuracy by the action of $\mathcal{D}_N$ [36, Ch. 5]. In that event, direct approximation of the term $\mathcal{D}\, u$ in (2) would have led to the matrix-vector product (in an obvious notation) $\mathbf{D}_N\, \mathbf{u}_N$ in the pre-transformed system from which (17) was derived. Here, the differentiation matrix $\mathbf{D}_N$ is given by

$$(\mathbf{D}_N)_{i,j} = L'_{j,N}(y_{i,N})\,, \qquad i,j = 1, \ldots, N\,. \tag{24}$$

To proceed, note that $L_{j,N}(x)$ in (13) may be written in the more succinct form

$$L_{j,N}(x) = \frac{p_N(x)}{(x - y_{j,N})\, p'_N(y_{j,N})}\,, \tag{25}$$

in which $p_N(x)$ is the *monic* polynomial with roots $y_{j,N}$. Then (24) and (25) yield

$$(\mathbf{D}_N)_{i,j} = \begin{cases} \dfrac{p'_N(y_{i,N})}{(y_{i,N} - y_{j,N})\, p'_N(y_{j,N})}\,, & i \neq j \\[2ex] \dfrac{p''_N(y_{j,N})}{2p'_N(y_{j,N})}\,, & i = j\,. \end{cases} \tag{26}$$

Because the nodes are presently based on Gauss-Legendre distributions in order to optimise the accuracy of the quadrature (15)—specifically, the monic polynomials $p_N(x)$ are as given in (53)–(55) below—the expressions in (26) cannot be obtained in closed form. Though one may use elegant asymptotic and numerical methods to approximate the roots of Legendre-based polynomials $p_N(x)$ (see, e.g., [37, 23, 30, 25]), the (partial) victory is Pyrrhic because the subsequent evaluation in (26) cannot yield closed-form expressions that are uniformly valid throughout $x \in [-1, 1]$.

In [37, 23, 30, 25] and related literature, roots of the Legendre polynomials of the first kind are calculated as either perturbations or iterations of the initial estimate $y_{j,N} = -\cos((4j-1)/(4N+2)\pi)$[1]; that is, in monic form,

$$p_N(x) = \widetilde{P}_N(x) \equiv \frac{2^N (N!)^2}{(2N)!}\, P_N(x) \quad \text{and} \quad y_{j,N} \approx -\cos((4j-1)/(4N+2)\pi)\,. \tag{27}$$

Theoretical progress can be made in an approximate sense by considering the qualitative similarities of differentiation matrices constructed via (26) using the Chebyshev polynomials of the first kind, for which

$$p_N(x) = \widetilde{T}_N(x) \equiv 2^{1-N}\, T_N(x) \quad \text{and} \quad y_{j,N} = -\cos((2j-1)/(2N)\pi)\,, \tag{28}$$

and for which (26) yields differentiation-matrix elements in closed form. Figure 1 demonstrates both qualitative and quantitative similarities of differentiation matrices $\mathbf{D}_N$ in (26) evaluated using both (27) and (28), for two values of N. Figure 2 shows the relative and absolute errors of the corresponding elements in the Legendre and Chebyshev differential matrices. The similarities and small errors (for the largest-magnitude elements) give credence to the use of the closed-form Chebyshev differentiation matrix for interpreting the behaviour arising in the non-closed-form Legendre case. However, it is well-known [12, 7, 6] that, in spite of the use of exact formulae in (26), the Chebyshev differentiation matrix (CDM) is in practice ill-conditioned due to the combination of roundoff errors and matrix operations. That is, direct discretisation of the differential form of FIDE (2) yields a potentially ill-conditioned system matrix in (17). Though differentiation-matrix accuracy can be improved at first [14] and higher [17] order, this aspect is considered no further since discrete differentiation is circumvented in the present VFIE approach.

[1] In which the minus sign is consistent with the node ordering at the start of this section.

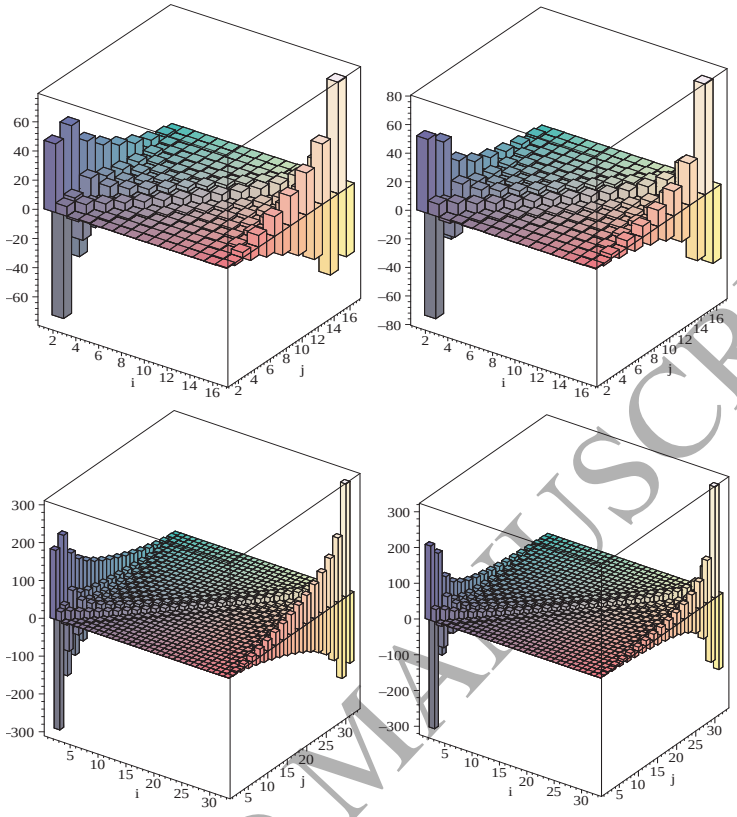

Figure 1: Pictorial representations of differentiation matrices constructed via (26) with monic Legendre ((27), left) and Chebyshev ((28), right) polynomials for $N = 16$ (top) and $N = 32$ (bottom). Vertical axes show $(\mathbf{D}_N)_{i,j}$ and demonstrate the qualitative and quantitative similarities resulting from the two nodal-distributions. Note that the Legendre implementation uses not the approximate nodes indicated in (27) but rather the numerically computed pseudo-exact ones.

Specifically, using (26) and (28), one can show explicitly that the CDM elements with the largest magnitude are, without error,

$$(\mathbf{D}_N)_{1,2} = -(\mathbf{D}_N)_{N,N-1} = \frac{2\sin\dfrac{3\pi}{2N}}{\sin\dfrac{2\pi}{N} - 2\sin\dfrac{\pi}{N}}\,. \tag{29}$$

Large-N asymptotics then yield an estimate of the CDM elemental supremum norm as

$$\|\mathbf{D}_N\|_\infty \sim \frac{3N^2}{\pi^2} - \frac{3}{8} + O(N^{-2})\,, \qquad N \to \infty\,, \tag{30}$$

and hence the CDM entries increase as $O(N^2)$ whereas the elements of the system matrix $\mathbf{M}_N$ in (17) remain well-conditioned, at order $O(1)$, as N increases, thereby strongly advocating adoption of the present differentiation-free approach.

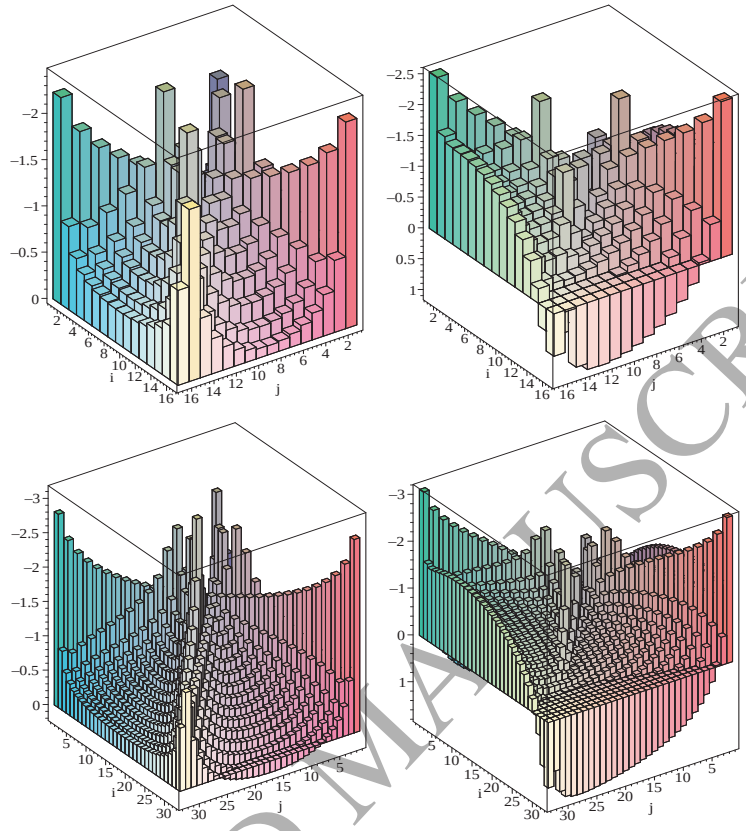

Figure 2: Pictorial representations of the relative (left) and absolute (right) errors in the Legendre and Chebyshev differentation matrices $\mathbf{D}_N$ portrayed in Figure 1 for $N = 16$ (top) and $N = 32$ (bottom). Vertical axes show $\log_{10}$ errors and have been inverted for clarity, so that smaller errors are denoted by taller elemental blocks.

4. Error Analysis

A theoretical analysis of the error incurred in computing u_N is now presented. Though a basic consideration of errors appears in the VFIE approach in [29], it not only computes the Volterra component of the VFIE crudely using Simpson's rule, but also concerns only convergence rates of $\|v - v_N\|$ (NB and not $\|u - u_N\|$) using a known exact solution. By contrast, the present work computes both Volterra and Fredholm components of the VFIE to spectral accuracy and, moreover, determines explicit error bounds for $\|u - u_N\|$ using only the approximate derivative v_N of the numerical solution u_N. The error analysis is now presented for cases 1 and 2 given in (21) and (22) respectively.

Case 1

Defining the linear operators $\mathcal{S}$ and $\mathcal{S}_N$ as

$$\mathcal{S} \equiv \frac{\mathcal{V}}{\mu} - \lambda\,\mathcal{F} \quad \text{and} \quad \mathcal{S}_N \equiv \frac{\mathcal{V}_N}{\mu} - \lambda\,\mathcal{F}_N\,, \tag{31}$$

the exact solution (11) of VFIE (7) can be written as

$$v = g + \mathcal{S}\, v \tag{32}$$

and the numerical solution (19) of (11) can be written as

$$v_{_N} = g + \mathcal{S}_{_N}\, v_{_N}\,. \tag{33}$$

Subtraction of (33) from (32) yields

$$v - v_{_N} = \mathcal{S}\, v - \mathcal{S}_{_N}\, v_{_N} = \mathcal{S}\,(v - v_{_N}) + (\mathcal{S} - \mathcal{S}_{_N})\, v_{_N}\,. \tag{34}$$

Since $v = \mathcal{D}\, u$ and $v_{_N} = \mathcal{D}\, \widetilde{u}_{_N}$, (34) can be rearranged to yield

$$(\mathcal{I} - \mathcal{S})\, \mathcal{D}\,(u - \widetilde{u}_{_N}) = (\mathcal{S} - \mathcal{S}_{_N})\, v_{_N}\,,$$

giving an explicit error formula for the exact solution u of the FIDE (1) as

$$u - \widetilde{u}_{_N} = (\mathcal{D} - \mathcal{S}\,\mathcal{D})^{-1}\big((\mathcal{S} - \mathcal{S}_{_N})\, v_{_N}\big)\,,$$

yielding the error bound

$$\|u - \widetilde{u}_{_N}\| \le C\, \sigma_{_N}\,, \tag{35}$$

where

$$C = \big\|(\mathcal{D} - \mathcal{S}\,\mathcal{D})^{-1}\big\| \quad \text{and} \quad \sigma_{_N} = \|(\mathcal{S} - \mathcal{S}_{_N})\, v_{_N}\|\,. \tag{36}$$

The term $\sigma_{_N}$ can be expressed via (33) as

$$\sigma_{_N} = \|\mathcal{S}\, v_{_N} - v_{_N} + g\|\,, \tag{37}$$

which demonstrates that the error is proportional to the residual obtained when the numerical solution $v_{_N}(x)$ is inserted into the exact VFIE (7). Alternatively, via (31), a bound on $\sigma_{_N}$ can be obtained as

$$\sigma_{_N} \le \frac{\|(\mathcal{V} - \mathcal{V}_{_N})\, v_{_N}\|}{\|\mu\|} + |\lambda|\, \|(\mathcal{F} - \mathcal{F}_{_N})\, v_{_N}\| \tag{38}$$

in which $\|(\mathcal{V} - \mathcal{V}_{_N})\, v_{_N}\|$ is obtained from the definition of $\mathcal{V}_{_N}$, which gives

$$(\mathcal{V} - \mathcal{V}_{_N})\, v_{_N}(x) = \mathcal{V}\,(\mathcal{I} - \mathcal{L}_{_N})\, v_{_N}(x) = \frac{\mathcal{V}\, p_{_N}(x)}{N!}\, v_{_N}^{(N)}(\eta)\,, \quad \eta \in (-1, 1)\,, \tag{39}$$

wherein $p_{_N}(x)$ is the monic polynomial whose roots are the N nodes $y_{i,_N}$, i.e.

$$p_{_N}(x) = \prod_{i=1}^{N} (x - y_{i,_N})\,. \tag{40}$$

Therefore, in (39), there results

$$\|(\mathcal{V} - \mathcal{V}_{_N})\, v_{_N}\| \le Q_{_N}\, \|v_{_N}^{(N)}\| = Q_{_N}\, \|\widetilde{u}_{_N}^{(N\,+\,1)}\|\,, \tag{41}$$

in which

$$Q_{\scriptscriptstyle N} \equiv \frac{\|\mathcal{V}\, p_{\scriptscriptstyle N}(x)\|}{N!}\,; \tag{42}$$

moreover, by standard Gaussian quadrature results [27],

$$\|(\mathcal{F} - \mathcal{F}_{\scriptscriptstyle N})\, v_{\scriptscriptstyle N}\| \le \psi_{\scriptscriptstyle N}^{(\nu)}\, \mathbb{F}_{2N\,-\,\nu}\,, \tag{43}$$

in which [21]

$$\psi_{\scriptscriptstyle N}^{(\nu)} \sim \frac{2^{2\nu\,-\,1}\sqrt{\pi}}{N^{(1\,-\,2\nu)/2}} \left(\frac{\mathrm{e}}{4N}\right)^{2N}\,,\quad N\to\infty \quad \text{and} \quad \mathbb{F}_{\scriptscriptstyle M} = \max_{x,y\in[-1,1]} \left|\frac{\partial^{\scriptscriptstyle M}}{\partial y^{\scriptscriptstyle M}}\big(k(x,y)\, v_{\scriptscriptstyle N}(y)\big)\right|, \tag{44}$$

in which ν corresponds to the number of endpoints included in the distribution, i.e. $\nu = 0,\ 1$ and 2 for Legendre, Radau and Lobatto nodes respectively. Combining (38), (41) and (43) yields

$$\sigma_{\scriptscriptstyle N} \le \frac{Q_{\scriptscriptstyle N}\, \big\|v_{\scriptscriptstyle N}^{(N)}\big\|}{\|\mu\|} + |\lambda|\, \psi_{\scriptscriptstyle N}^{(\nu)}\, \mathbb{F}_{2N\,-\,\nu}. \tag{45}$$

With $\sigma_{\scriptscriptstyle N}$ in (35) bounded by (45), the constant C given by (36) can be bounded via

$$C = \Big\|\big((\mathcal{I} - \mathcal{S})\, \mathcal{D}\big)^{-1}\Big\| = \|\mathcal{D}^{-1}\, (\mathcal{I} - \mathcal{S})^{-1}\| = \|\mathcal{V}\, (\mathcal{I} - \mathcal{S})^{-1}\| \le \|\mathcal{V}\|\, \|(\mathcal{I} - \mathcal{S})^{-1}\|\,, \tag{46}$$

in which, adopting the approach of Atkinson [3, Eqns. (4.1.13)–(4.1.17)], $\|\mathcal{V}\|$ is computed as

$$\|\mathcal{V}\| = \|\mathcal{V}\, 1\| = \max_{x\in[-1,1]} |x+1| = 2\,.$$

By (31), operators $\mathcal{S}$ and $\mathcal{S}_{\scriptscriptstyle N}$ are linear combinations of $\mathcal{V}$, $\mathcal{F}$, $\mathcal{V}_{\scriptscriptstyle N}$ and $\mathcal{F}_{\scriptscriptstyle N}$, for which, by the definitions of Lagrangian interpolation and Gaussian quadrature respectively, $(\mathcal{V} - \mathcal{V}_{\scriptscriptstyle N})\, v(x) \to 0$ and $(\mathcal{F} - \mathcal{F}_{\scriptscriptstyle N})\, v(x) \to 0$ as $N\to\infty$ for all $v\in\mathcal{C}$ and $x\in[-1,1]$. That is, $\mathcal{S}_{\scriptscriptstyle N}\, v$ is pointwise uniformly convergent to $\mathcal{S}\, v$ as $N\to\infty$ for all $v\in\mathcal{C}$ and $x\in[-1,1]$, and hence, by [3, Thm 4.1.2] and [24, Eq. (4.7.17b)], $(\mathcal{I} - \mathcal{S})^{-1}$ in (46) exists and is uniformly bounded by

$$\big\|(\mathcal{I} - \mathcal{S})^{-1}\big\| \le \frac{1 + \big\|(\mathcal{I} - \mathcal{S}_{\scriptscriptstyle N})^{-1}\big\|\, \|\mathcal{S}\|}{1 - \big\|(\mathcal{I} - \mathcal{S}_{\scriptscriptstyle N})^{-1}\big\|\, \|(\mathcal{S} - \mathcal{S}_{\scriptscriptstyle N})\, \mathcal{S}\|}\,, \tag{47}$$

the denominator of which is positive by construction. The sub-elements on the right-hand side of (47) are computed using the approach in Atkinson [3, Eqns. (4.1.13)–(4.1.17)], which gives $\|\mathcal{S}\|$ as

$$\|\mathcal{S}\| = \|\mathcal{S}\, 1\| \equiv \|s\|\,,$$

say, in which $s(x)$ is given by (9), (10) and (31) as

$$s(x) = \frac{x+1}{\mu(x)} - \lambda \int_{-1}^{1} k(x,y)\, dy\,. \tag{48}$$

Similarly, $\|(\mathcal{S} - \mathcal{S}_{\scriptscriptstyle N})\, \mathcal{S}\|$ in (47) is computed as

$$\|(\mathcal{S} - \mathcal{S}_{\scriptscriptstyle N})\, \mathcal{S}\| = \|(\mathcal{S} - \mathcal{S}_{\scriptscriptstyle N})\, \mathcal{S}\, 1\| = \|(\mathcal{S} - \mathcal{S}_{\scriptscriptstyle N})\, s\|$$

and $\|(\mathcal{I}-\mathcal{S}_N)^{-1}\|$ as

$$\|(\mathcal{I}-\mathcal{S}_N)^{-1}\| = \|(\mathcal{I}-\mathcal{S}_N)^{-1}\,1\| \equiv \|r_N\|\ ,$$

say, in which $r_N(x)$ is the solution of

$$r_N - \mathcal{S}_N\, r_N = 1\,,$$

whose left-hand side is of the same form as VFIE (33). Consequently, nodal values of $r_N(x)$ are found by solving a linear system with the same matrix as in (17), i.e.

$$(\mathbf{I}_N - \mathbf{M}_N)\,\mathbf{r}_N = \mathbf{1}\,, \tag{49}$$

in which $\mathbf{I}_N$ and $\mathbf{M}_N$ are as given in (18) and the entries of the vectors $\mathbf{r}_N$ and $\mathbf{1}$ are given by

$$\{\mathbf{r}_N\}_i = r_N(y_{i,N}) \quad \text{and} \quad \{\mathbf{1}\}_i = 1\,, \quad i=1,\ldots,N\,.$$

It is noted that, for the purposes of efficiency, (17) and (49) can be solved in the partitioned form

$$(\mathbf{I}_N - \mathbf{M}_N)\,(\mathbf{v}_N|\mathbf{r}_N) = (\mathbf{g}_N|\mathbf{1})\,.$$

Solving (49) gives the nodal vector $\mathbf{r}_N$, the elements of which are used in the Nyström inversion formula

$$r_N(x) = 1 + \sum_{j=1}^{N}\left\{\frac{\tau_{j,N}(x)}{\mu(x)} - \lambda\, w_{j,N}\, k(x,y_{j,N})\right\} r_N(y_{j,N})\,,$$

from which $\|r_N\|$ can be computed directly; similarly, $\|s\|$ can be computed directly from (48). Finally, (35), (37) and (46) give the case-1 theoretical bound

$$\|u-\widetilde{u}_N\| \le \frac{2\,(1+\|r_N\|\,\|s\|)}{1-\|r_N\|\,\|(\mathcal{S}-\mathcal{S}_N)\,s\|}\,\|\mathcal{S}\,v_N - v_N + g\| \tag{50}$$

on the (case-1) error $u-\widetilde{u}_N$ that is explicitly computable in terms of only the derivative v_N of the case-1 numerical solution $\widetilde{u}_N$.

Case 2

Subtraction of (22) from (21) and addition of $u-u=0$ to the resulting left-hand side gives a bound on the case-2 error as

$$\widetilde{u}_N - u + u - \widehat{u}_N = (\mathcal{V}-\mathcal{V}_N)v_N \Rightarrow \|u-\widehat{u}_N\| \le \|u-\widetilde{u}_N\| + \|(\mathcal{V}-\mathcal{V}_N)\,v_N\|$$

which, by (41) and (50), yields

$$\|u-\widehat{u}_N\| \le \frac{2\,(1+\|r_N\|\,\|s\|)}{1-\|r_N\|\,\|(\mathcal{S}-\mathcal{S}_N)s\|}\,\|\mathcal{S}\,v_N - v_N + g\| + Q_N\|v_N^{(N)}\|\,. \tag{51}$$

As the case-2 solution arises when $v_N(x)$ is not integrable, the bound (51) is not computable as the operator $\mathcal{S}$ contains the Volterra operator $\mathcal{V}$ via (31). Therefore, the term $\|\mathcal{S}\,v_N - v_N + g\|$ in (51)—defined as σ_N in

(37)—must be bounded using (45). Similarly, as $\mathcal{S}\, s$ will in general be uncomputable, a bound (analogous to (45)) on $\|(\mathcal{S} - \mathcal{S}_{N})\, s\|$ can be found as

$$\|(\mathcal{S} - \mathcal{S}_{N})\, s\| \leq \frac{Q_{N}\|s^{(N)}\|}{\|\mu\|} + |\lambda|\ \psi_{N}^{(\nu)}\, \mathbb{S}_{2N\,-\,\nu}\,,$$

in which

$$\mathbb{S}_{M} = \max_{x,y\in[-1,1]} \left| \frac{\partial^{M}}{\partial y^{M}} \big(k(x,y)\, s(y)\big) \right| .$$

Collecting results, the computable case-2 error bound is given by

$$\|u - \widehat{u}_{N}\| \leq \frac{2\ (1 + \|r_{N}\|\, \|s\|)\ \big(Q_{N}\big\|v_{N}^{(N)}\big\| + |\lambda|\|\mu\|\, \psi_{N}^{(\nu)}\, \mathbb{F}_{2N\,-\,\nu}\big)}{\|\mu\| - \|r_{N}\|\ \big(Q_{N}\|s^{(N)}\| + |\lambda|\|\mu\|\, \psi_{N}^{(\nu)}\, \mathbb{S}_{2N\,-\,\nu}\big)} + Q_{N}\, \|v_{N}^{(N)}\| \,. \tag{52}$$

Computable error bounds (50) and (52) have now been derived for the general FIDE (2). Attention now turns to the derivation of exact formulae for computing Q_{N} in bound (52).

4.1. Explicit Formula for $\mathbf{Q}_{N}$

As stated after (15), the above error analysis can be implemented using Gauss-Legendre (Legendre), Legendre-Gauss-Radau (Radau) or Legendre-Gauss-Lobatto (Lobatto) nodal distributions, for which the factor Q_{N} defined in (42) can be found explicitly. Recall that $\nu = 0,\ 1$ and 2 for Legendre, Radau and Lobatto nodes respectively. Then the monic polynomials (40) associated with each distribution are given by the explicit formulae

$$p_{N}^{(0)}(x) = \frac{2^{N}(N!)^{2}}{(2N)!} P_{N}(x)\,, \tag{53}$$

$$p_{N}^{(1)}(x) = \frac{2^{N}(N!)^{2}}{(2N)!}\ (P_{N\,-\,1}(x) - P_{N}(x))\ , \tag{54}$$

and

$$p_{N}^{(2)}(x) = \frac{2^{N}(N!)^{2}}{(2N)!} \frac{2N-1}{N(N-1)} (x^{2}-1)\, P'_{N\,-\,1}(x)\,, \tag{55}$$

in which only the Radau polynomial containing $x = -1$ is considered as results for $x = 1$ can be derived from $p_{N}^{(1)}(-x)$, which yields the same value of Q_{N}. First note that, using the Legendre polynomial relationships

$$\frac{(x^{2}-1)\, P'_{N}(x)}{N} = x\, P_{N}(x) - P_{N\,-\,1}(x)$$

and

$$(2N+1)\, x\, P_{N}(x) = (N+1)\, P_{N\,+\,1}(x) + N\, P_{N\,-\,1}(x)\,,$$

(55) can be rewritten as

$$p_{N}^{(2)}(x) = \frac{2^{N}(N!)^{2}}{(2N)!}\ (P_{N}(x) - P_{N\,-\,2}(x))\ , \tag{56}$$

using which (53), (54) and (56) have the general form

$$p_{N}^{(\nu)}(x) = \frac{2^{N}(N!)^{2}}{(2N)!} \left((1 + \nu - \nu^{2})\, P_{N-\nu}(x) + \frac{\nu(3-(-1)^{\nu})}{4}\, P_{N}(x) \right) . \tag{57}$$

Using now the Legendre polynomial relationship

$$(2N+1)\,P_{N}(x) = \frac{d}{dx}\left(P_{N+1}(x) - P_{N-1}(x)\right)\,,$$

integration of (57) using (9) and subsequent use of the definition (42) gives the bound

$$Q_N^{(\nu)} \le \frac{2^N N!}{(2N)!}\left(\frac{\|P_{N+1-\nu} - P_{N-1-\nu}\|}{2(N-\nu)+1} + \frac{\nu(3-(-1)^\nu)}{4}\frac{\|P_{N+1} - P_{N-1}\|}{2N+1}\right)\,, \tag{58}$$

because $|1+\nu-\nu^2| = 1$ for $\nu = 0,\ 1$ and 2. To compute the bound (58) note that, when N is even,

$$\|P_N - P_{N-2}\| = |P_N(0) - P_{N-2}(0)|\,, \tag{59}$$

so that, using the Legendre-polynomial definition

$$P_N(x) = 2^N \sum_{i=0}^{N} \binom{N}{i}\binom{\frac{N+i-1}{2}}{N} x^i\,,$$

there results

$$P_N(0) = \frac{2^N\left(\frac{N-1}{2}\right)!}{\left(-\frac{(N+1)}{2}\right)!\,N!}\,,$$

which, augmented by the Gamma-function definitions

$$\Gamma\left(\tfrac{1}{2}+N\right) = \left(-\tfrac{1}{2}+N\right)! = \frac{(2N)!\sqrt{\pi}}{4^N\,N!} \quad\text{and}\quad \Gamma\left(\tfrac{1}{2}-N\right) = \left(-\tfrac{1}{2}-N\right)! = \frac{(-4)^N\,N!\sqrt{\pi}}{(2N)!}\,,$$

yields the explicit formula

$$P_N(0) = \frac{(-1)^{N/2}N!}{2^N\left[\left(\frac{N}{2}\right)!\right]^2}\,. \tag{60}$$

Therefore, by (59) and (60),

$$\|P_N - P_{N-2}\| = \frac{(2N-1)\,N!}{(N-1)\,2^N\left[\left(\frac{N}{2}\right)!\right]^2} \tag{61}$$

for N even. Because when N is odd, (59) no longer holds, an exact bound similar to (61) cannot then be found. Using Stirling's formula, (61) becomes

$$\|P_N - P_{N-2}\| \sim \frac{2N-1}{N-1}\sqrt{\frac{2}{N\pi}}\,, \quad N(\text{even}) \to \infty\,. \tag{62}$$

Indeed, an exact relationship of the form (59) cannot be derived for odd N, for which the value of $\widehat{x}_N$, say, in

$$\|P_N - P_{N-2}\| = |P_N(\widehat{x}_N) - P_{N-2}(\widehat{x}_N)|\,,$$

cannot be expressed in terms of N. However, it transpires (as confirmed numerically below) that (62) is in practice a good asymptotic approximation of $\|P_N - P_{N-2}\|$ for all N. Therefore, (58) and (62) yield the asymptotic prediction $\widetilde{Q}_N^{(\nu)}$ of the bound on $Q_N^{(\nu)}$

$$\widetilde{Q}_N^{(\nu)} \sim \frac{1}{\sqrt{\pi}}\left(\frac{\mathrm{e}}{2N}\right)^N\left(\frac{1}{(N-\nu)\sqrt{N+1-\nu}} + \frac{\nu(3-(-1)^\nu)}{4N\sqrt{N+1}}\right)\,, \quad N\to\infty\,. \tag{63}$$

In Figure 3 are presented plots, corroborating this assertion, of exact spatial-distribution moduli $|Q_N^{(\nu)}(x)|$ (bounded by (58)) and asymptotic bounds $\widetilde{Q}_N^{(\nu)}$ (63) for $\nu = 0,\ 1$ and 2 and for $N = 9$ and 10, for both values of which the bounds are seen to be accurate; more so for $\nu = 0$ (Legendre) and $\nu = 2$ (Lobatto) than for $\nu = 1$ ((left) Radau). An alternative form of this corroboration is presented for only $\nu = 0$ in Figure 4, which reveals that asymptotic formula (63) is extremely accurate for both even and odd N of order as low as $O(1)$.

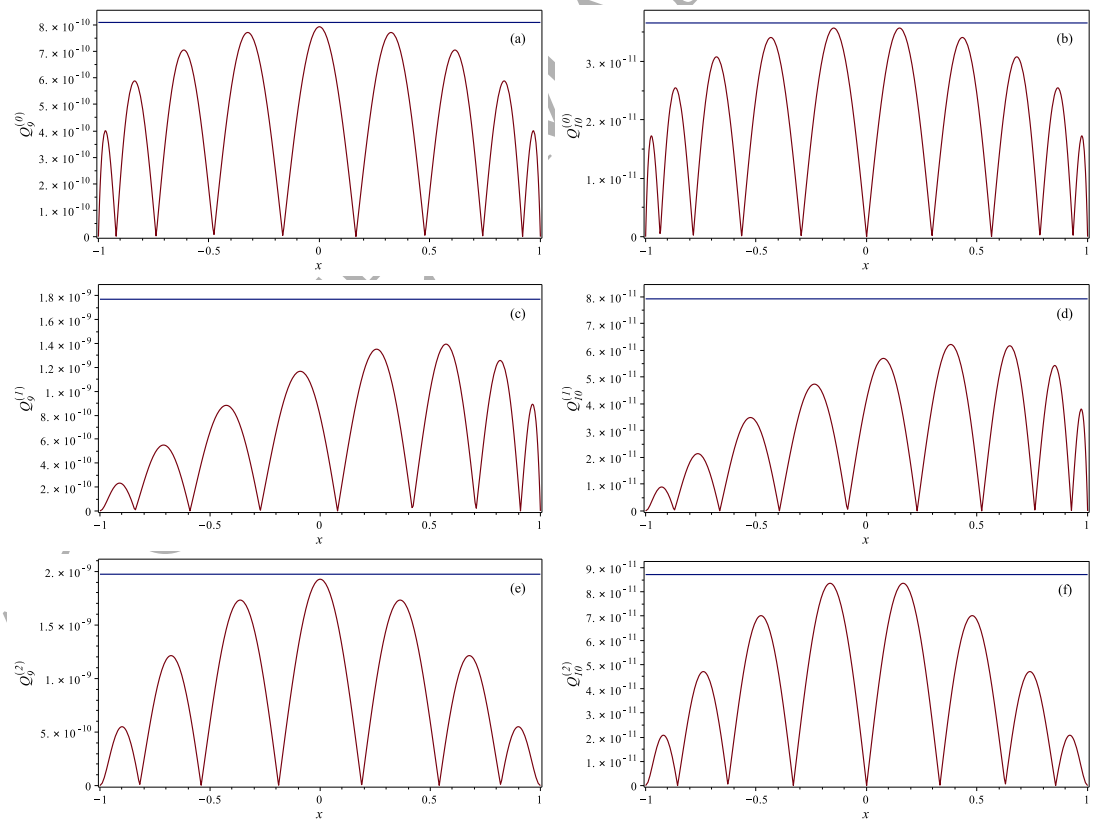

Figure 3: Exact values of $|Q_N^{(\nu)}(x)|$ for $x \in [-1, 1]$ (curves) and asymptotic bounds $\widetilde{Q}_N^{(\nu)}$ (63) (horizontal lines) for $N = 9$ (left column) and $N = 10$ (right column) and $\nu = 0,\ 1$ and 2 (top, medium and bottom rows). The plots demonstrate two things: first, that (63) is a good approximating formula for both even and odd N; second, that the large-N asymptotic predictions are accurate even for moderate values of N.

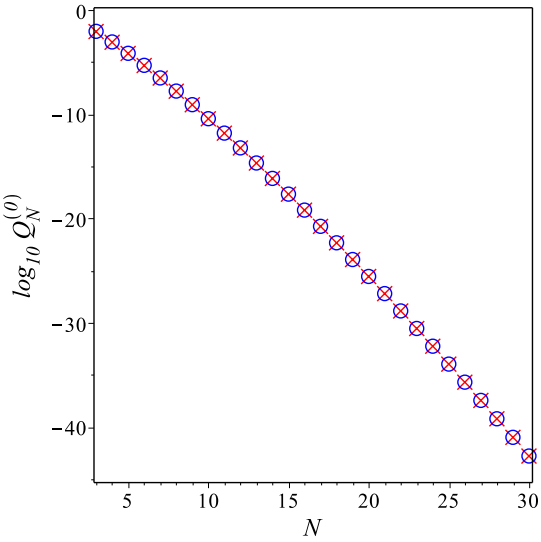

Figure 4: Exact values of $\left\|Q_N^{(0)}\right\|$ (blue circles) compared with asymptotic formula $\widetilde{Q}_N^{(0)}$ (63) (red crosses); results for $\nu = 1$ and $\nu = 2$ are qualitatively identical. The large-N asymptotic predictions are seen in this depiction to be accurate even for low values of N.

4.2. Asymptotic Convergence Rates

Using the asymptotic rates (44) and (63), for $\psi_N^{(\nu)}$ and $\widetilde{Q}_N^{(\nu)}$ respectively, there results

$$\frac{\psi_N^{(\nu)}}{\widetilde{Q}_N^{(\nu)}} \sim \frac{\pi\,(4N)^{(2\nu+1)/2}\,(N-\nu)\,\sqrt{(N+1)^2-\nu(N+1)}}{4N\,\sqrt{N+1}+\nu(3-(-1)^\nu)\,(N-\nu)\,\sqrt{N+1-\nu}}\,\left(\frac{\mathrm{e}}{8N}\right)^N\,, \tag{64}$$

in which the asymptotic condition "$N \to \infty$" is here and subsequently relaxed as a result of the observations drawn from Figure 4. Analysis of (64) reveals that $\psi_N^{(\nu)}/\widetilde{Q}_N^{(\nu)} \sim O(N^{-N})$, whence (45) may be approximated by

$$\sigma_N \leq \frac{\widetilde{Q}_N^{(\nu)}\left\|v_N^{(N)}\right\|}{\|\mu\|}$$

so that, by (35), the asymptotic error convergence rate for case 1 is

$$\|u-\widetilde{u}_N\| \sim \widetilde{Q}_N^{(\nu)}\|v_N^{(N)}\|\,. \tag{65}$$

Following a similar argument, the asymptotic error convergence rate (52) for case 2 is also given by (65), with $\widetilde{u}_N$ replaced by $\widehat{u}_N$; consequently, both are henceforth replaced by u_N. Because by construction the denominator in (47) must be positive, the predicted rate (65) for both cases is therefore valid provided that

$$\|v_N^{(N)}\| \sim o(N^N) \quad \text{and} \quad \mathbb{F}_{2N-\nu} \sim o(N^{2N})\,. \tag{66}$$

By (65) the error $u - u_N$ in the exact solution u of FIDE (2) is predicted explicitly in terms of the numerical solution v_N of approximate VFIE (19), where $u_N' = v_N$. By contrast, in the independent approach adopted in [21] (hereafter referred to as case 0), the error in u is given explicitly not by v_N but by

the numerical solution, $\overline{u}_N$ say, of the approximation

$$\overline{u}_N - \mu\,\mathcal{D}_N\,\overline{u}_N - \lambda\,\mathcal{K}_N\,\overline{u}_N = f\,, \tag{67}$$

of (2), in which $\mathcal{D}_N$ is the symbolic representation of the differentiation operator $\mathcal{D}$ acting on $\mathcal{L}_N$ defined in (12). In [21], the error $u - \overline{u}_N$ is shown to have the asymptotic error-convergence rate

$$\|u - \overline{u}_N\| \sim \phi_N^{(\nu)} \|\overline{u}_N^{(N)}\|\,,$$

in which the factor $\phi_N^{(\nu)}$ arises through numerical differentiation; it has the asymptotic form

$$\phi_N^{(\nu)} \sim \frac{2^{\nu-3/2}}{N^{(\nu^2\,-\,\nu\,-\,4)/2}} \left(\frac{\mathrm{e}}{2N}\right)^N. \tag{68}$$

Therefore by (63) and (68), as $N \to \infty$,

$$\frac{\widetilde{Q}_N^{(\nu)}}{\phi_N^{(\nu)}} \sim \frac{N^{(\nu^2\,-\,\nu\,-\,4)/2}}{2^{\nu\,-\,3/2}\,\sqrt{\pi}} \left(\frac{1}{(N-\nu)\,\sqrt{N+1-\nu}} + \frac{\nu(3-(-1)^\nu)}{4N\,\sqrt{N+1}}\right) \sim N^{(\nu^2\,-\,\nu\,-\,7)/2}\,, \tag{69}$$

and so $\phi_N^{(\nu)} > \widetilde{Q}_N^{(\nu)}$ for all N so that, provided that both norms $\|v_N^{(N)}\|$ and $\|\overline{u}_N^{(N)}\|$ are of the same order, by (63) and (68) the case 0, case 1 and case 2 errors are predicted to converge at the same rate as $N \to \infty$. Additionally, by (69), the case 1 and case 2 errors are predicted to be uniformly lower than the case 0 errors incurred in [21].

5. Numerical Results

Using the algebraic manipulator `Maple`, the methods and bounds derived above were respectively implemented and validated on four test problems, each with known solutions, chosen to demonstrate the accuracy of the theory on potentially challenging problems. The components of each test problem are shown in Table 1. As the results were qualitatively similar for each nodal distribution, only the results for the Legendre distribution, for which $\nu = 0$, are presented.

Figure 5 shows that, for each test problem, the case-1 errors are lower than the case-2 errors and so, as expected, it is more accurate to integrate the numerical VFIE solution exactly to obtain the FIDE solution

Problem	Type	Solution $u(x)$	$\mu(x)$	Kernel $K(x,y)$	λ
1	Smooth	$\sin x + x^2$	$\sec x$	$(x^3-1)\,y\cos y$	$\frac{1}{3}$
2	Runge	$\frac{1}{1+25x^2}$	$\frac{1}{x-2}$	$(x+1)(y^2-5)$	$-\frac{1}{2}$
3	Steep	e^{15x}	e^{x}	e^{x+y}	1
4	Oscillatory	$\cos 12x$	$\frac{1}{x^5-3x+1}$	$\sin x\,y^3$	2

Table 1: Test problems with solutions of four qualitatively distinct forms. The Runge phenomenon [10, 11], extreme gradient and high-frequency oscillations, in the solutions of problems 2, 3 and 4 respectively, offer well-documented challenges to approximation methods.

rather than to integrate its Lagrange interpolant. Additionally, as predicted at the end of Section 4.2, the new case-1 and case-2 errors are smaller in magnitude than the case-0 errors incurred in [21], confirming that bypassing the need for numerical differentiation by converting from FIDE to VFIE form yields a more accurate numerical solution.

Figure 5 also reveals that the case-1 error bound is more accurate (by comparison with the actual computed errors) than the case-2 error bound, particularly for problem 2 in which the case-2 error bound diverges whilst the true errors converge with increasing N: this divergence, and the large discrepancy between true case-2 errors and error bounds for the other problems, is due to the terms $\left\|v_N^{(N)}\right\|$ and $\mathbb{F}_{2N-\nu}$ in the error bound (52). Via the mean-value theorem used to derive (39), the truncation parameter $\eta \in (-1, 1)$ that yields the true error $(\mathcal{V} - \mathcal{V}_N)\, v_N$ is unknown, so $v_N^{(N)}(\eta)$ must be replaced by $\left\|v_N^{(N)}\right\|$, the latter of which may be much greater than the former. The same argument applies to the Gaussian-quadrature error term (43), which includes the unknown values of x and y in (44); as these are unknown, $\mathbb{F}_{2N-\nu}$ must be computed by maximising over $x, y \in [-1, 1]$, and so the quadrature error may also be over-estimated.

6. Conclusions

A novel method for the accurate numerical solution of one-dimensional, first-order Fredholm integro-differential equations has been developed by first converting the problem into a Volterra-Fredholm integral equation. The technique has been validated on diverse and challenging test problems. A novel error analysis has been conducted and validated to yield explicitly computable (using only the numerical solution) error bounds that predict true computational errors to spectral accuracy. Two independent sub-approaches have been analysed depending upon whether or not intermediate stages of the novel process admit exact integration. For both cases, errors are shown theoretically and numerically to be smaller in magnitude than the errors incurred by a previous approach [21].

References

[1] O. A. Arqub, M. Al-Smadi and N. Shawagfeh, *Solving Fredholm integro–differential equations using reproducing kernel Hilbert space method*, Appl. Math. Comput., 219 (2013), 8938–8948.

[2] E. Aruchunan and J. Sulaiman, *Quarter-sweep Gauss-Seidel method for solving first order linear Fredholm integro-differential equations*, Matematika, 27 (2011), 199–208.

[3] K. E. Atkinson, *The Numerical Solution of Integral Equations of the Second Kind*, Cambridge University Press, Cambridge, UK, 1997.

[4] E. Babolian and L. M. Delves, *A fast Galerkin scheme for linear integro-differential equations*, IMA J. Numer. Anal., 1 (1981), 193–213.

[5] E. Babolian, M. T. Kajani and M. Ghasemi, *Numerical solution of linear integro-differential equation by using sine–cosine wavelets*, Appl. Math. Comput., 180 (2006), 569–574.

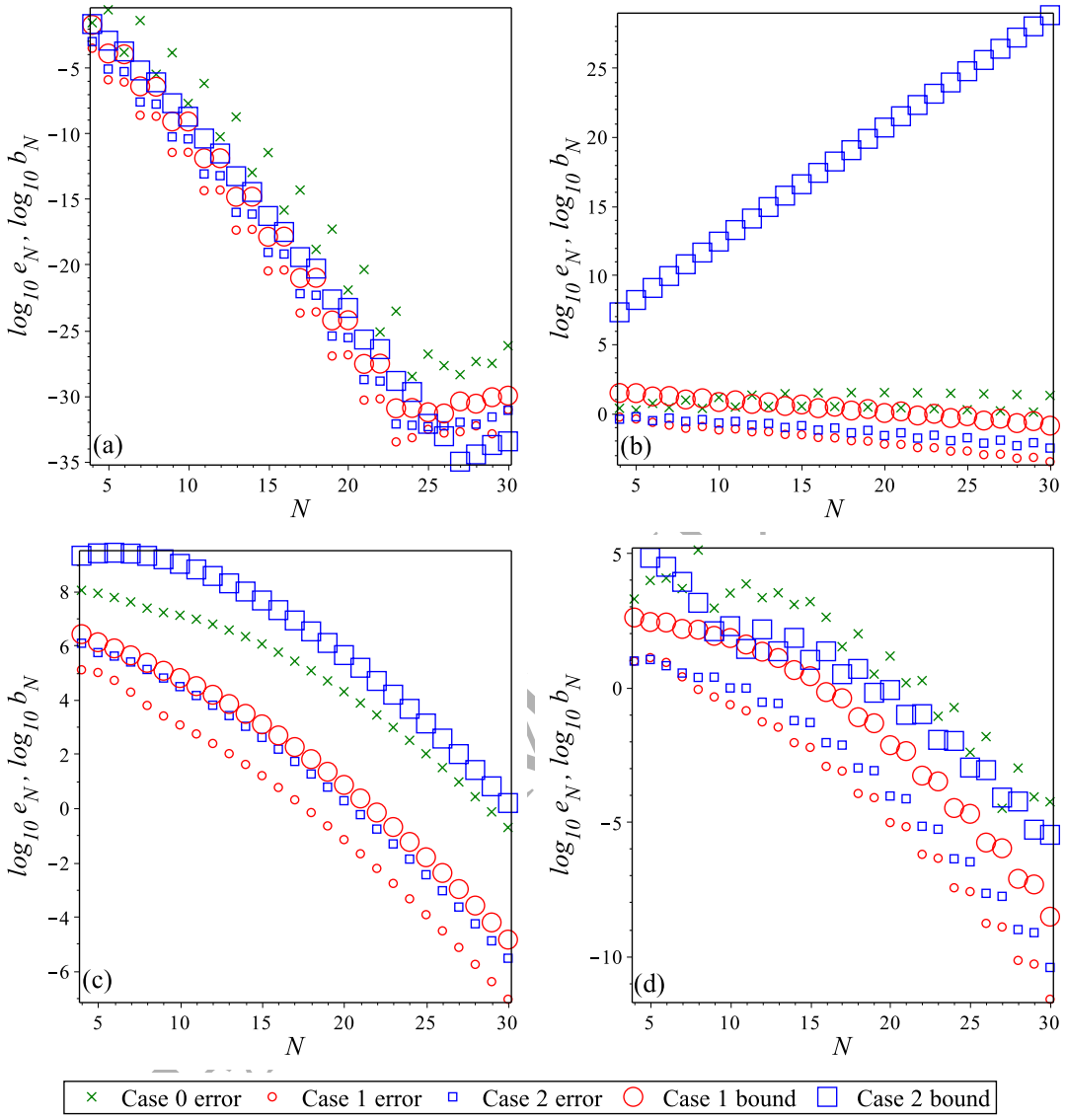

Figure 5: Logarithmic plots showing convergence or divergence with N of error $e_N = ||u - u_N||$ and bound b_N given by (50) and (52), for cases 0, 1 and 2 for each of problems (a) 1 "smooth", (b) 2 "Runge", (c) 3 "steep" and (d) 4 "oscillatory". All computations are conducted on Legendre nodes, i.e. $\nu = 0$. Note the divergence of the case-2 bound for the Runge problem, as discussed in the text. In all four problems, the new case-1 and case-2 errors are smaller than those incurred in [21].

[6] R. BALTENSPERGER AND J.-P. BERRUT, *The errors in calculating the pseudospectral differentiation matrices for Čebyšev-Gauss-Lobatto points*, Comput. Math., Appl., 37 (1999), 41–48.

[7] A. BAYLISS, A. CLASS AND B. J. MATKOWSKY, *Roundoff error in computing derivatives using the Chebyshev matrix*, J. Comput. Phys., 116 (1994), 380–383.

[8] N. BILDIK, A. KONURALP AND S. YALÇINBAŞ, *Comparison of Legendre polynomial approximation and variational iteration method for the solutions of general linear Fredholm integro-differential equations*, Comput. Math.

Appl., 59 (2010), 1909–1917.

[9] A. H. BORZABADI AND M. HEIDARI, *A successive numerical scheme for some classes of Volterra-Fredholm integral equations*, Iranian Journal of Mathematical Sciences and Informatics, 10 (2015), 1–10.

[10] J. P. BOYD, *Defeating the Runge Phenomenon for equispaced polynomial interpolation via Tikhonov regularization*, Appl. Math. Lett., 5 (1992), 57–59.

[11] J. P. BOYD, *Exponentially accurate Runge-free approximation of non-periodic functions from samples on an evenly spaced grid*, Appl. Math. Lett., 20 (2007), 971–975.

[12] K. S. BREUER AND R. M. EVERSON, *On the errors incurred calculating derivatives using Chebyshev polynomials*, J. Comput. Phys., 99 (1992), 56–67.

[13] Z. CHEN AND W. JIANG, *An approximate solution for a mixed linear VolterraFredholm integral equation*, Appl. Math. Lett., 25 (2012), 1131–1134.

[14] B. COSTA AND W. S. DON, *On the computation of high order pseudospectral derivatives*, Appl. Num. Math., 33 (2000), 151–159.

[15] P. DARANIA AND A. EBADIAN, *A method for the numerical solution of the integro-differential equations*, Appl. Math. Comput., 188 (2007), 657–668.

[16] H. LAELI DASTJERDI AND F. M. MAALEK GHAINI, *Numerical solution of Volterra–Fredholm integral equations by moving least square method and Chebyshev polynomials*, Appl. Math. Model., 36 (2012), 3283–3288.

[17] W. S. DON AND , *Accuracy enhancement for higher derivatives using Chebyshev collocation and a mapping technique*, SIAM J. Sci. Comput. , 18 (1997), 1040–1055.

[18] A. I. FAIRBAIRN AND M. A. KELMANSON, *Computable theoretical error bounds for Nyström methods for Fredholm integral equations of the second kind*. In *Proc. 10th UK Conf. on Boundary Integral Methods*, 85–94, 2015.

[19] A. I. FAIRBAIRN AND M. A. KELMANSON, *An exponentially convergent Volterra-Fredholm method for integro-differential equations*. In *Proc. 11th UK Conf. on Boundary Integral Methods*, 53–63, 2017.

[20] A. I. FAIRBAIRN AND M. A. KELMANSON, *Spectrally accurate Nyström-solver error bounds for 1-D Fredholm integral equations of the second kind*, Appl. Math. Comput., 315 (2017), 211–223.

[21] A. I. FAIRBAIRN AND M. A. KELMANSON, *A priori Nyström-method error bounds in approximate solutions of 1-D Fredholm integro-differential equations*, submitted to Int. J. Mech. Sci., 2018.

[22] M. FATHY, M. EL-GAMEL AND M. S. EL-AZAB, *Legendre-Galerkin method for the linear Fredholm integro-differential equations*, Appl. Math. Comput., 243 (2014), 789–800.

[23] L. GATTESCHI, *Sull'approssimazione asintotica degli zeri dei polinomi sferici ed ultrasferici*, Boll. Unione Mat. Ital. Ser. 3, 5(3/4) (1950), 305–313.

[24] W. HACKBUSCH, *Integral Equations: Theory and Numerical Treatment*, Birkhäuser Verlag, Basel, Switzerland, 1995.

[25] N. HALE AND A. TOWNSEND, *Fast and accurate computation of Gauss-Legendre and Gauss-Jacobi quadrature nodes and weights*, SIAM J. Sci. Comput., 35(2), (2013), A652–A674.

[26] F. A. HENDI AND A. M. ALBUGAMI, *Numerical solution for Fredholm–Volterra integral equation of the second kind by using collocation and Galerkin methods*, Journal of King Saud University - Science, 22 (2010), 37–40.

[27] F. B. HILDEBRAND, *Introduction to Numerical Analysis*, McGraw-Hill, New York, 1974.

[28] S. M. HOSSEINI AND S. SHAHMORAD, *Tau numerical solution of Fredholm integro-differential equations with arbitrary polynomial bases*, Appl. Math. Model., 27 (2003), 145–154.

[29] P. LINZ, *A method for the approximate solution of linear integro-differential equations*, SIAM J. Numer. Anal., 11 (1974), 137–144.

[30] F. G. LETHER, *On the construction of Gauss-Legendre quadrature rules*, J. Comp. Appl. Math., 4(1) (1978), 47–52.

[31] K. MALEKNEJAD AND M. ATTARY, *An efficient numerical approximation for the linear class of Fredholm integro-differential equations based on Cattani's method*, Commun. Nonlinear Sci. Numer. Simulat., 16 (2011), 2672–2679.

[32] M. M. MUSTAFA AND I. N. GHANIM, *Numerical solution of linear Volterra-Fredholm integral equations using Lagrange polynomials*, Mathematical Theory and Modeling, 4 (2014), 137–146.

[33] S. NEMATI, *Numerical solution of Volterra–Fredholm integral equations using Legendre collocation method*, J. Comput. Appl. Math., 278 (2015), 29–36.

[34] J. RASHIDINIA AND M. ZAREBNIA, *The numerical solution of integro-differential equation by means of the Sinc method*, Appl. Math. Comput., 118 (2007), 1124–1130.

[35] P. K. SAHU AND S. RAY, *Legendre spectral collocation method for Fredholm integro-differential equation with variable coefficients and mixed conditions*, Appl. Math. Comput., 268 (2015), 575–580.

[36] L. N. TREFETHEN, *Spectral Methods in* MATLAB, SIAM, Philadelphia, 2000.

[37] F. G. TRICOMI, *Sugli zeri dei polinomi sferici ed ultrasferici*, Ann. Mat. Pura Appl., 31 (1950), 93–97.

[38] M. A. WOLFE, *The numerical solution of non-singular integral and integro-differential equations by iteration with Chebyshev series*, Comput. J., 12 (1969), 193–196.

[39] S. YALÇINBAŞ AND M. SEZER, *The approximate solution of high-order linear volterra-fredholm integro-differential equations in terms of taylor polynomials*, Appl. Math. Comput., 112 (2000), 291–308.

[40] S. YALÇINBAŞ, M. SEZER AND H. H. SORKUN, *Legendre polynomial solutions of high-order linear Fredholm integro-differential equations*, Appl. Math. Comput., 210 (2009), 334–349.